

## **DEVELOPMENT OF A LOW-COST ANALYZER FOR MISALIGNMENT IDENTIFICATION BASED ON VIBRATION AND CURRENT ANALYSIS**

**Dedi Suryadi<sup>1\*</sup>, Acraz M. Bahrum<sup>2</sup>, Novalio Daratha<sup>3</sup>, Radzi Ambar<sup>4</sup>**

Department of Mechanical Engineering, University of Bengkulu, Bengkulu, Indonesia<sup>12</sup>

Department of Electrical Engineering, University of Bengkulu, Bengkulu, Indonesia<sup>3</sup>

Department of Electronic Engineering, Universiti Tun Hussein Onn Malaysia, Batu Pahat, Malaysia<sup>4</sup>

dedi\_suryadi@unib.ac.id

Received: 09 July 2024, Revised: 31 October 2024, Accepted: 02 November 2024

\*Corresponding Author

### **ABSTRACT**

*This paper proposes a low-cost analyzer based on vibration and motor current signature analysis (MCSA) using the Arduino microcontroller. Misalignment identification on induction motors with disc coupling is considered a case study. Several methods for misalignment identification have already been conducted in previous research. However, there are still issues with making the identification more reliable and well-known for further investigation. This paper describes the design and development of an analyzer for misalignment identification that is easy to use and fast utilizing a low-cost Arduino microcontroller. Furthermore, this experimental rig also consists of several additional components such as; an induction motor, shaft, and bearing dan disk coupling. In this paper, misalignment distance variables were set in 0 mm, 0.5 mm, 1 mm, and 1.5 mm, and the motor speed was varied from 500 rpm to 1500 rpm with an increment of 100 rpm. The misalignment characteristic was experimentally achieved using an analyzer with two sensors: an accelerometer for vibration analysis and a current sensor for MCSA. As a result, a low-cost analyzer for misalignment has been successfully developed. The results show that misalignment was explicitly defined by dominant peak frequencies at 3X rpm for vibration analysis and side bands around the main frequency for MCSA. Moreover, side-band frequency increases by increasing the misalignment distance.*

**Keywords:** Current Signature Analysis, Misalignment, Microcontroller, Sensor, Vibration

### **1. Introduction**

Misalignment commonly occurs on the rotating machinery due to improper machine assembly, thermal distortion on the machine, the asymmetry of the applied load, and uneven base (Jang & Khonsari, 2015). Misalignment affects the destruction of part of a rolling, sealing, and connection (Verma et al, 2014). Misalignment can also generate an eccentricity in the air gap in the electric motor, making it possible to damage the rotor and stator (Devarajan et al, 2021; Suryadi et al, 2018; Suryadi et al, 2019; Suryadi et al, 2021).

The damage appearing on the rotor causes the age of spare parts to become shorter due to the uneven distribution of forces on mechanical components (Harris & Barnsy, 2001). Research showed that the damage previously mentioned can be avoided by handling and early detection of damage to the machine, known as the predictive maintenance process (Suryadi & Vetrano, 2019; Scheffer & Girdhar, 2004; Prayoga & Suryadi 2018). In the normal predictive maintenance analysis process, damage can be diagnosed by looking at the signal characteristics of vibration experienced by machines (Sinha, 2008; Chen, 2011; Suryadi & Pratama, 2020).

Various techniques are available to diagnose misalignment on rotating machinery; some are vibration-based signal processing and Motor Current Signature Analysis (MCSA). The technique of vibration-based signal processing is the most common diagnostic method; each condition produces a distinctive vibration pattern and provides information about the machine's condition (Chen, 2011). A vibration-based signal technique is one of the most important techniques for diagnosing problems in rotating machinery (Rai & Upadhyay, 2016) (Kumar et al, 2018). Hence, the motor current signal monitoring and analysis can be performed by the MCSA method to directly determine the mechanical and electrical failures in induction motors (Thomson & Fenger, 2001). MCSA method is done by analyzing the current signals to determine the condition of the motor stator (Miljkovic, 2015; Calis, 2014).

Another study related to the detection of mechanical faults on three-phase motors also defined the achievement of the method, the MCSA used in mechanical fault identification artificially. Also, it analyzed the vibration signal using MATLAB (Verucchi et al, 2016). A study was also done using the diagnostic media MCSA and vibration signals and concluded that this MCSA alone could predict the effects of misalignment without using the vibration signal by using a representation of the orbit plot. Results from the study showed that the misalignment could be detected with an orbit plot (Verma et al, 2014). The study demonstrated a mechanism in which the power transmission between the motor and the load carried by various types of couplings is most often used in the industry. The results of this study indicate that the fault indicator is highly dependent on the features of the coupling itself (Bossio et al, 2009) (WU et al, 2019). A study in (Saavedra & Ramirez, 2022) conducted model simulations for analysis and direct experiments to diagnose misalignment angles in induction motors. Results from the study indicate that the misalignment angle can be detected from a variable electric motor but with a difficult diagnosis. This study is equipped with vibration analysis and thermography.

This study will develop a low-cost analyzer for misalignment on an induction motor that can identify misalignment on a rotor system based on both signal analysis and MCSA. Cheap hardware is selected to develop an analyzer equipped with a microcontroller. Hardware data acquisition (DAQ), an Arduino microcontroller, and an ADS1256 analog-to-digital converter (ADC) with a 24bits resolution as a system data acquisition instrument are used to identify misalignment in induction motors with vibration analysis and current in the induction motor. ADXL335 accelerometer is a vibration sensor and SCT-013 is a current sensor that is an open-source sensing unit and can be supported by a microcontroller. This research will be conducted to get information on the characteristics of the vibration signal and the current signal to the misalignment condition.

## 2. Methodology

This research uses a model of a dynamic rotor system that helps adjust misalignment conditions. The model consists of a 3-phase induction motor, steel shaft, bearings, and steel disc coupling. The 3-phase induction motor is connected to a steel shaft supported by two UCF and UCT bearing types. These bearings are placed at the center and the end of the rotor, as illustrated in Figure 1.

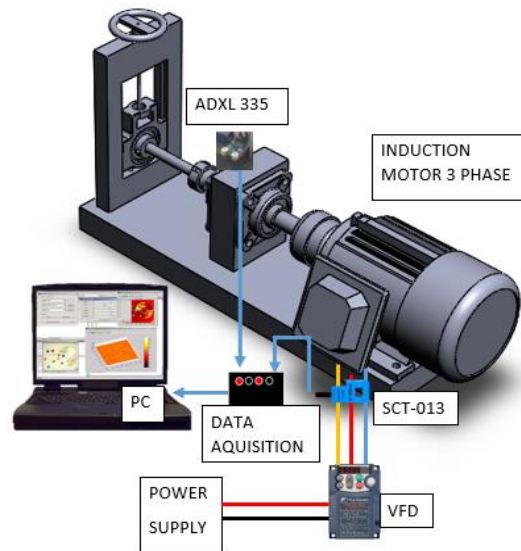


Fig. 1. Test rig

In this study, signal characteristics are captured simultaneously by both the ADXL335 accelerometer sensor and the SCT-013 current sensor. The ADXL335 accelerometer sensor is attached over the radial direction of the axis of a UCF bearing to measure vibration. At the same time, the SCT-013 current sensor is attached to one of the 3-phase cables connected to the variable frequency drive (VFD), which adjusts the motor's rotation. The Accelerometer dan current sensors are calibrated to standard ones before being used for analyzer.

The concept of system modeling is that the device works by adjusting the parallel bearing alignment, where distance is measured using a dial indicator. Distances between bearings are varied: 0 mm (alignment condition), 0.5 mm, 1 mm, and 1.5 mm. The distance variation value is measured by a dial indicator with various distances X, as in Figure 2.

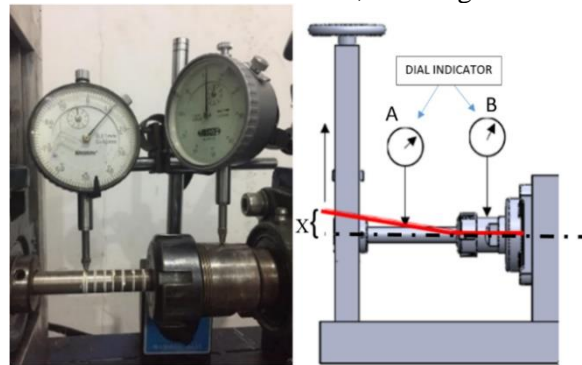


Fig. 2. Misalignment Model

The sensors (vibration and current) were connected to a data acquisition system that processed the data and conveyed it to a PC. Data entered by the PC in analog data is converted to digital signals to be analyzed. The data acquisition system was created using a combination of Arduino UNO and an ADS1256 ADC. The wiring diagram is shown in Figure 3. The 24-bit ADS1256 ADC is chosen because it is more efficient compared to the ADC inside Arduino UNO. Analog values output of the ADC is read by a PC using SPI communication (Serial Peripheral Interface) in binary numbers.

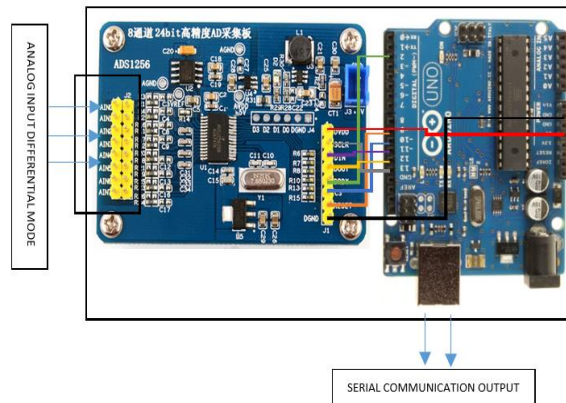


Fig. 3. Wiring Diagram of Data Acquisition

Data is collected at a rate of 2,800 samples per second. For data retrieval, a serial monitor on a PC is used, and the number of samples for the vibration sampling is 4096 points or about 1.5 seconds of measurements. Furthermore, the current sampling used 32768 points with a time of about 11.7 seconds. The collected data from both the accelerometer and the current sensor are transformed using the Fast Fourier Transform (FFT) with a hanging window to see the dominant characteristic's peak.

### 3. Results and Discussion

The developed DAQ system has been calibrated. First, calibration is conducted for the accelerometer and current sensor to compare measurements of developed devices and standard tools. Here, acceleration and current values are obtained by varying motor speed from 500 to 1500 rpm with increments of 100 rpm. The error values of the vibration and the current measurements are presented in Tables 1 and 2, respectively.

Table 1 - Error Value of RMS Vibration Measurement Standard and Data Acquisition Device

Motor Speed (RPM)	RMS Measurement Standard (mm/s)	Data Acquisition Device RMS Value (mm/s)	Error (%)
500	1.03	1.06	3.59
600	1.47	1.48	1.29
700	1.67	1.51	9.35

800	2.23	2.31	3.72
900	2.43	2.42	0.08
1000	2.8	2.84	1.71
1200	2.87	2.93	2.33
1300	3.6	3.58	0.5
1400	3.63	3.62	0.24
1500	3.86	4.00	3.73
1600	4.63	4.70	1.59
<b>Average</b>			<b>2.56</b>

Table 2 - Error Value of RMS Value Current Measurement Standards and Data Acquisition

Motor Speed (RPM)	RMS Measurement Standard	Data Acquisition	
	Device (A)	Device RMS Value (A)	Error (%)
500	1.55	1.58	1.90
600	1.57	1.59	1.44
700	1.61	1.60	0.33
800	1.60	1.62	1.28
900	1.61	1.62	0.70
1000	1.60	1.64	2.57
1200	1.59	1.66	4.46
1300	1.67	1.68	0.87
1400	1.76	1.74	1.28
1500	1.78	1.78	0.59
1600	1.83	1.79	1.91
<b>Average</b>			<b>2.56</b>

Table 1 shows that the average error for vibration measurement is 2.56%. On the other hand, Table 2 shows the average error for the current measurement is 1.58%. Hence, from these results, it can be concluded that the proposed misalignment analyzer device can be used in vibration and current analyses and extended experiments. According to the International Electrotechnical Commission (IEC) 13B-23, the maximum error that can be accepted as a sensor for panels is  $\pm 5\%$ .

Furthermore, the data acquisition system can measure the current and vibration in the form of an analog signal, process it into digital signals, and then process it on a PC for analysis. The results of the designed data acquisition system can be seen in Figure 3.1.

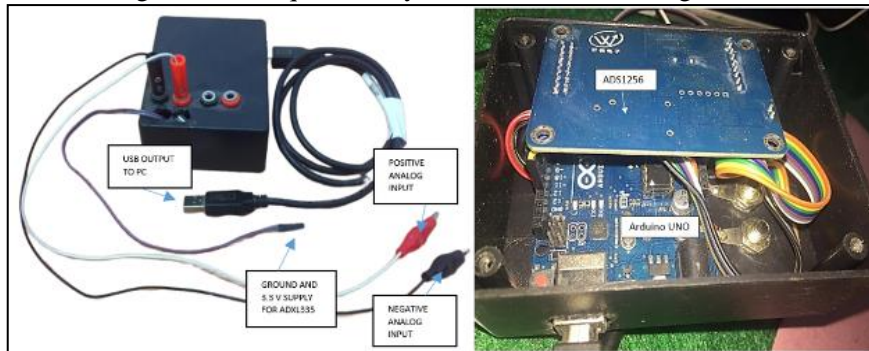


Fig. 3.1. The Data Acquisition System

### 3.1. Vibration Analysis

In this research, two case studies are considered; **Case A:** alignment, i.e., normal condition, and **Case B:** 0.5 mm, 1.0 mm, and 1.5 mm parallel misalignment conditions. In each case, the motor speed varies from 500 rpm to 1500 rpm with an increment of 100 rpm. Then the time domain data is taken for about 1.5 seconds with 4096 nodal obtained in the 100 Hz frequency range. The data was obtained in the time domain and then converted into frequency domain form to see the characteristics of each test conducted.

Variations were made on the distance of misalignment and then were adjusted by variations in the normal distribution. This data then derived the occurrence of misalignment conditions with a distance of 0.5 mm, 1 mm, and 1.5 mm by varying the rotation and length of the misalignment. This process was done to diagnose the actual damage. Furthermore, the

process continued to analyze the effect in the form of spectrum analysis on current and vibrations. Figure 5 shows the results of spectral map vibration analyses for Case A and Case B.

Figure 3.2(a) shows the spectrum corresponding to a normal condition in which no misalignment is present in the system. Two patterns can be observed. First, the dominant harmonics' magnitudes are almost zeros with increasing frequency. Second, the dominant frequency appears around 50 Hz. One can conclude that the dominant frequency is not affected by the engine rotation speed. Note that the carrier power frequency is about 50 Hz in Indonesia. A scale of 1.5 mm/s is hardly noticeable unless the frequency's dominant appears at 50 Hz.

Figures 3.2(b), 3.2(c), and 5(d) show that the spectrums are dominated by three major components: fundamental components ( $f_0$ ), second harmonics ( $2f_0$ ) and third harmonics ( $3f_0$ ). The fundamental frequency  $f_0$  is also equivalent to the rotation speed. For example, if the rotation is 1500 RPM, the frequency is 25 Hz. Furthermore, in terms of the magnitudes of the dominant frequencies. The figures also show that increasing the severity of misalignment corresponds to increasing magnitudes of those dominant components. The frequency component increases with the misalignment (Suryadi et al, 2021) and rotational speed (Li et al, 2001), even over the synchronous component 1X, which can be used to identify the misalignment fault. The previous results show that the spectrum's shape is affected by the severity of the misalignment and the rotational speed of the shaft. Consequently, vibration measurements can be used to detect misalignment on a rotating machine and evaluate the estimation of the corresponding severity.

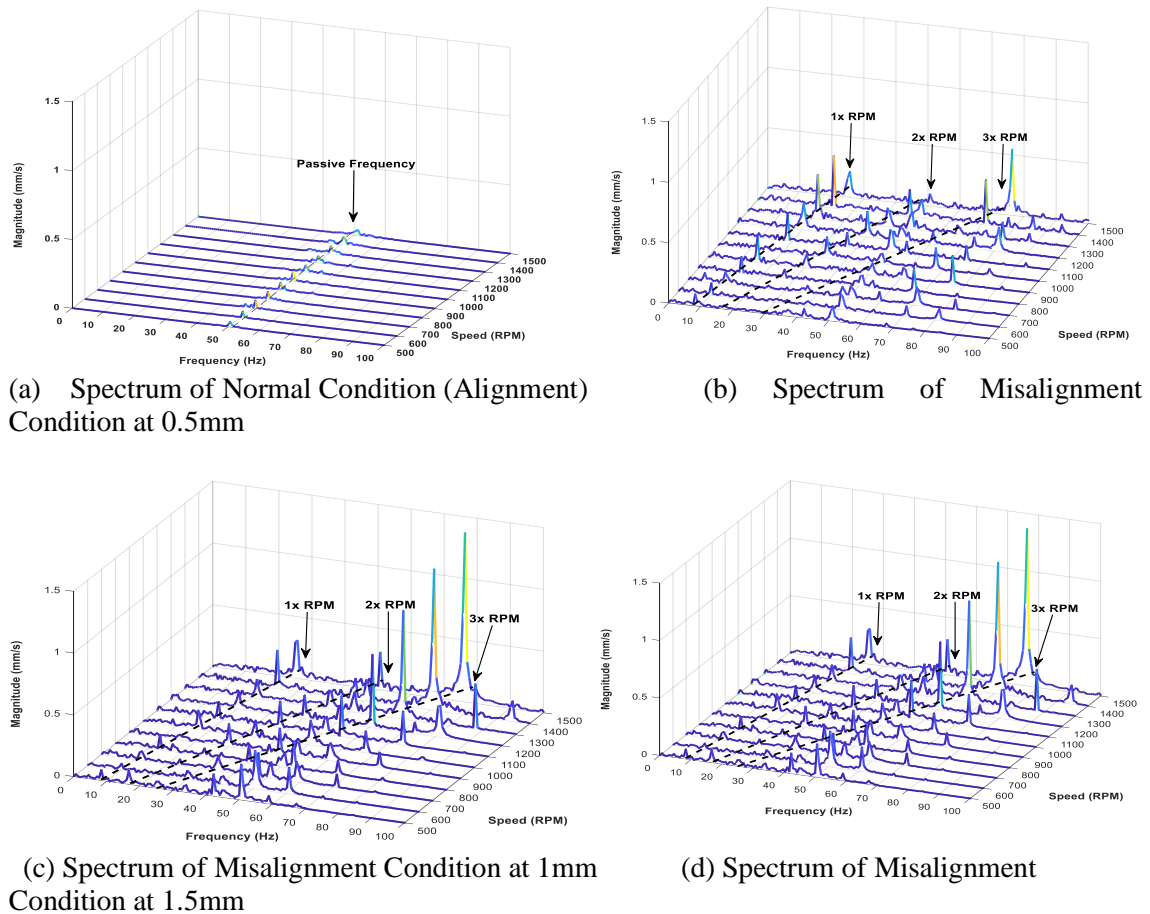


Fig. 1.2. Spectral Map Vibration Analysis for Case A (a) and Case B (b, c and d)

### 3.2. Motor Current Signature Analysis

In this study, there are eleven variations of effect misalignment. The speeds varied from 500 rpm to 1500 rpm in increments of 100 rpm. Analysis of the current response to each speed was recorded for about 11.7 seconds with 32768 nodes. This process is conducted to obtain a

response to the data in the time domain. Furthermore, these data were analyzed using a Fast Fourier Transform (FFT) to receive the response data in the frequency domain as shown in Figure 3.3.

The frequency of the motor supply current, rotor speed, and motor slip frequency component can be extracted from the frequency domain analysis of the motor current. Motor current is modulated by the speed of the rotor, and supply harmonics the big one. Therefore, the result shows that the speed of the motor appears as sidebands around the primary frequency. It also appears in the frequency of rotation on the motor denoted by  $f_r$ . Although, in theory, this sideband should not exist in this practice, the sideband supply current is induced in the motor because the motor is not completely symmetrical (in terms of electric or magnetic). These components can be seen in the stator current signal as in Figure 3.3. The magnitude of the elements of this eccentricity ( $f \pm f_r$ ) increases when the level of misalignment gets worse (Ganeriwala, 2024).

In the motor current signal, Figure 3.4 shows the sideband around the frequency components of motor rotation.

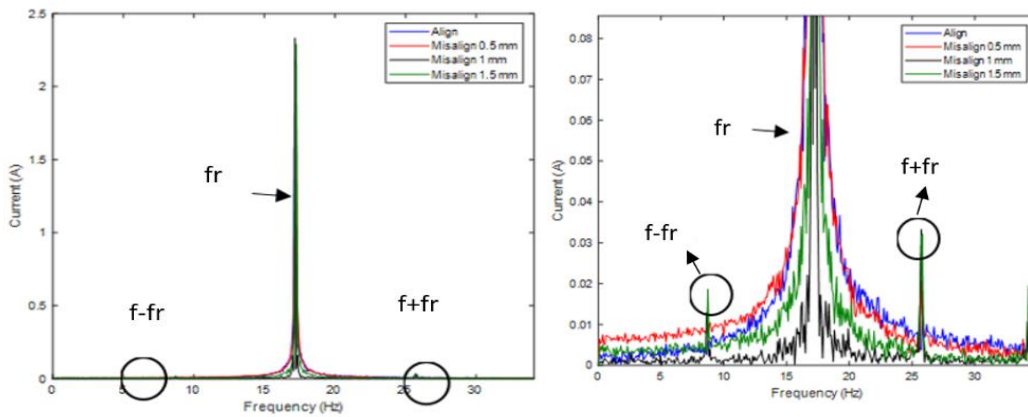
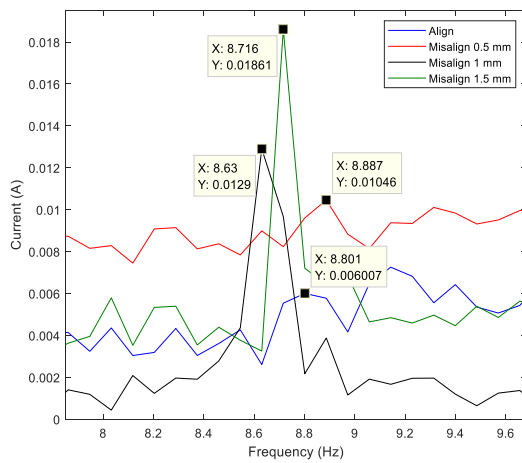
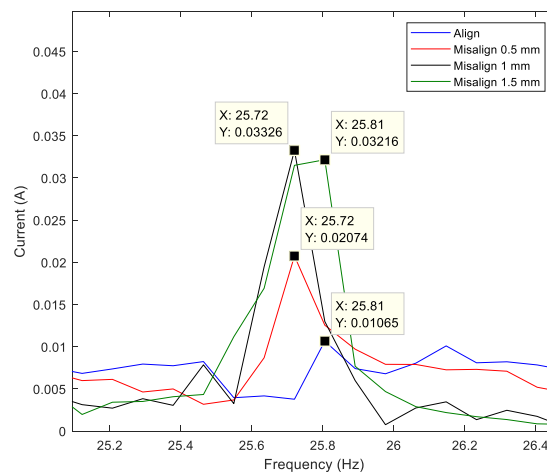


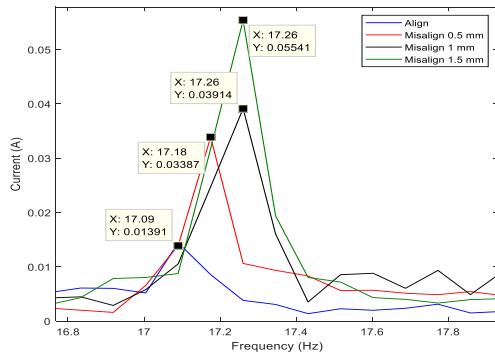
Fig. 3.3. Frequency Current Spectrum Analysis



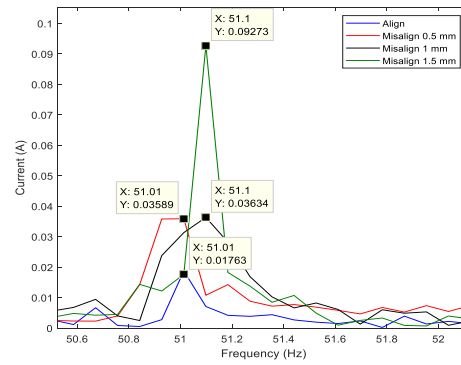
(a)  $f-fr$  Current Spectral at 500 rpm



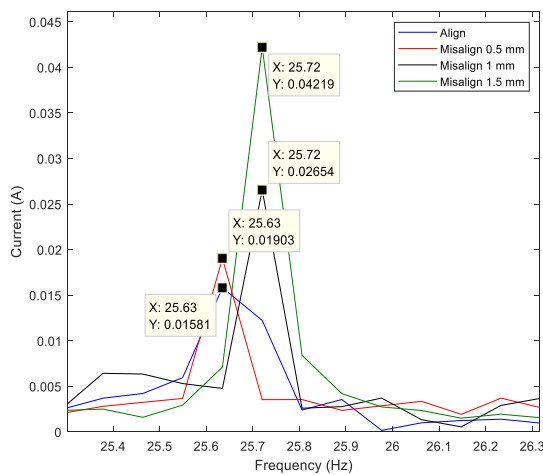
(b)  $f+fr$  Current Spectral at 500 rpm



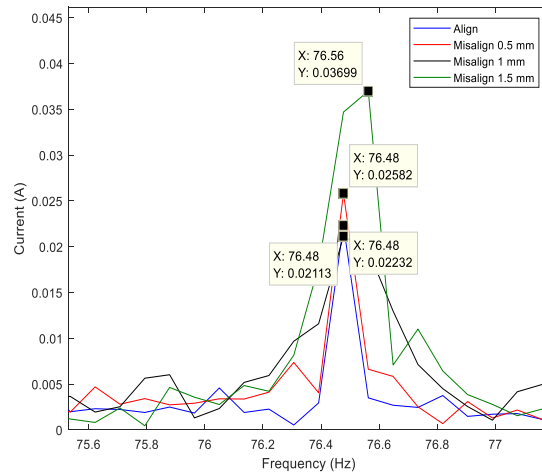
(c)  $f-fr$  Current Spectral at 1000 rpm



(d)  $f+fr$  Current Spectral at 1000 rpm



(e)  $f-fr$  Current Spectral at 1500 rpm



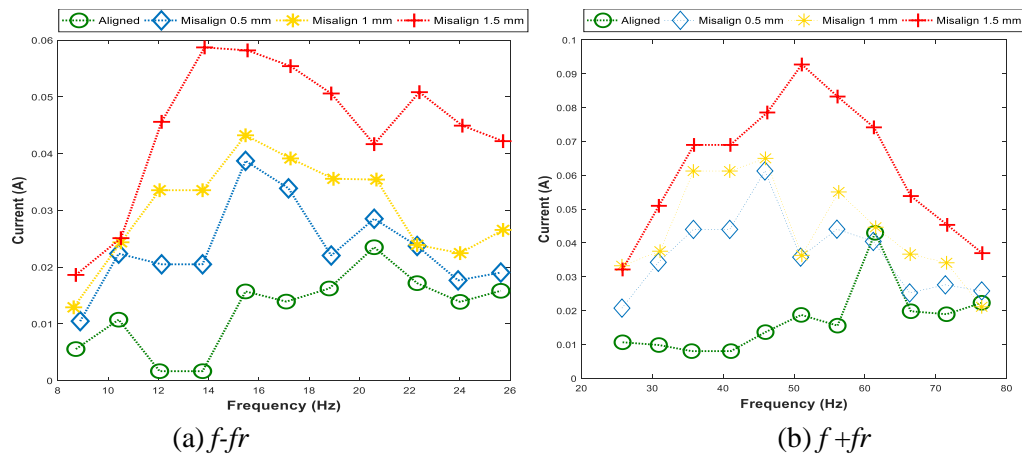
(f)  $f+fr$  Current Spectral at 1500 rpm

1500 rpm  
Fig. 3.4.  $f \pm fr$  Component

Figure 3.5 shows the comparison of the peak value of  $f \pm fr$  at any rpm. Spectral components with the current misalignment variation are at position alignment, 0.5 mm, 1 mm, and 1.5 mm. The speed is 500 to 1500 rpm in increments of 100 rpm. Any increase in the engine turns the peak of the primary frequency or frequency shift rotation following the rise of rpm.

The peak value of the components in the frequency shift  $f-fr$  with each increment into 11 variations were rotated from 500 rpm to 1500 rpm. Component  $f+fr$  frequency shift also occurs every increment of 11 variations in rotation from 500 rpm to 1500 rpm. These also occurred due to the severity's influence on misalignment.

Stator measurement shows that the current spectrum components at frequency  $f+fr$  and  $f-fr$  levels rise due to misalignment. The rotor speed modulates motor current, and there are a lot of harmonics that arise. Therefore, the rotor speed frequency appears as sidebands around the primary frequency. Although the theory that this sideband should not exist, in practice this sideband is induced in the supply current (stator) for the motor is not completely symmetrical electrically or magnetically. It has been verified experimentally that these components can be seen on the stator current signal as the magnitude of the components of this eccentricity ( $f \pm fr$ ) increases when the degree of misalignment increases. Sideband appears when there are misalignment and almost no sideband at standard conditions in the stator current component at frequency  $f \pm fr$  as the diagnosis of the fault of the electric motor (Carlos et al, 2016).

Fig. 3.5.  $f \pm fr$  Peak Value Plot

#### 4. Conclusion

Based on the performance analysis above, predictive maintenance monitoring tools have been successfully developed using both vibration and motor current motor analysis. In the case of misalignment conditions on rotor dynamics, misalignment is characterized by dominant frequencies of 3 rpm peak based on vibration analysis. The vibration level increases by increasing the misalignment level. Moreover, MCSA's characteristics are contained in the sideband of the left and right primary frequency on the stator current induction motor. Sideband will be increased according to the severity of interference due to misalignment conditions.

#### References

- Bossio, J. M., Bossio, G. R. & De Angelo, C. H. (2009). Angular misalignment in Induction Motors with Flexible Coupling. *35<sup>th</sup> Annual Conference of IEEE Industrial Electronics*. pp. 1033-1038.
- Carlos, V., José, B., Guillermo, B. & Gerardo, A. (2016). Misalignment detection in induction motors with flexible coupling by means of estimated torque analysis and MCSA. *Mechanical Systems and Signal Processing*, 80, 570-581. doi.org/10.1016/j.ymsp.2016.04.035.
- Calis, H. (2014). Vibration and motor current analysis of induction motors to diagnose mechanical faults. *Journal of Measurement in Engineering*, 2 (4), pp. 190-198.
- Chen, C. S. & Chen, J. (2011). Rotor fault diagnosis system based on individual sGA-based neural networks. *Expert Syst. Appl.*, 38, 10822-10830. Doi: 10.1016/j.eswa.2011.02.074.
- Devarajan, G., Chinnusamy, M. & Kaliappan, L. (2021). Detection and classification of mechanical faults of three phase induction motors via analysis of the thermal image pixels and adaptive neuro-fuzzy inference system. *Journal of Ambient Intelligence and Humanized Computing*, 12, 4619-4630. Doi: 10.1007 / s12652-020-01857-8.
- Ganeriwala, S. (2024). Induction Motor Diagnostics Using Vibration and Motor Current Signature Analysis. In: Allen, M., Blough, J., Mains, M. (eds) *Special Topics in Structural Dynamics & Experimental Techniques*, Volume 5. SEM 2023. Conference Proceedings of the Society for Experimental Mechanics Series. Springer, Cham. [https://doi.org/10.1007/978-3-031-37007-6\\_21](https://doi.org/10.1007/978-3-031-37007-6_21)
- Jang, J. Y., & Khonsari, M. M. (2015). On the characteristics of misaligned journal bearings. *Lubricants*, 3 (1), 27-53. Doi: 10.3390 / lubricants3010027.
- Kumar, S., Loksha, M., Kumar, K. & Srinivas, K. R. (2018). Based Vibration Fault Diagnosis Techniques for Rotating Mechanical Components. Review Paper. *IOP Conf. Ser. Mater. Sci. Eng.* 376 (1), 1-6. Doi: 10.1088 / 1757-899X / 376/1/012 109.
- Kumar, R., Singh, M., Khan, S. *et al.* (2023). A State-of-the-Art Review on the Misalignment, Failure Modes and Its Detection Methods for Bearings. *MAPAN* 38, 265-274. <https://doi.org/10.1007/s12647-022-00605-x>

- Li Z, Li J, Li M. (2018). Nonlinear dynamics of unsymmetrical rotor-bearing system with fault of parallel misalignment. *Advances in Mechanical Engineering*, 10(5). doi:10.1177/1687814018772908
- Miljkovic, D. (2015). Brief review of the motor current signature analysis. *IEEE Ind. Appl. Mag*, 5 (1), 14-26.
- Prayoga H. & Suryadi, D. (2018). Analisis LKarakteristik Vibrasi pada Paper Dryer Machine untuk Deteksi Dini Kerusakan Spherical Roller Bearing. *ROTASI*, 20 (2), 110-117. Doi. DOI: 10.14710/rotasi.20.2.110-117.
- Rai, A. & Upadhyay, S. (2016). A Review on Signal Processing Techniques utilized in the Fault Diagnosis of Rolling Element Bearings. *Tribology International*, 96, 289-306. Doi. 10.1016 / j.triboint.2015.12.037.
- Saavedra, P. N. & Ramírez, D. E. (2022). Vibration analysis of rotors for the identification of shaft misalignment Part 2. Experimental validation. *Proc. Inst. Mech. Eng. Part C J. Mech. Eng. Sci.*, 218, 987–999. Doi. 10.1243 / 0954406041991198
- Scheffer, C. & Girdhar, P. (2004). *Machinery Vibration Analysis and Predictive Maintenance*, Elsevier, Netherlands.
- Sinha, J. K. (2008). Vibration-based diagnosis techniques used in nuclear power plants. *An overview of experiences. Nuclear Engineering Design*, 238 (9), 2439-2452. Doi : 10.1016/j.nucengdes.2008.03.007.
- Suryadi, D., Meilianda, R., Suryono, A. & Munadi. (2018). Expert System for Identifying Industry Breakdown Method Using Certainty Factor. *ROTASI*, 20 (1), 56-62. Doi. 10.14710 / rotasi.20.1.
- Suryadi, D. & Vetrano, M. (2019). Identification of unbalance and Methods Balancing on Single Rotor by Using Digital Signal Analyzer (DSA). *SeNITiA*, Bengkulu, Indonesia, pp. 262-266.
- Suryadi D. & Pratama, M. D. (2020). Desain and Manufacture of Fault monitoring System based on Vibration Level. *REKAYASA MESIN*, 11 (1), 21-29. DOI: <https://doi.org/10.21776/ub.jrm.2020.011.01.3>.
- Suryadi, D., Febriyanto, M. R. & Fitrilina. (2021). Analysis of Misalignment on Rotor Dynamic using Sound Analysis. *REKAYASA MESIN*, 12 (2), 487-495. DOI: <https://doi.org/10.21776/ub.jrm.2021.012.02.25>
- Thomson, W. T. & Fenger, M. (2001). Current signature analysis to detect faults of induction motors. *IEEE Industry. Applications Magazine*, 7, 26-34. Doi : 10.1109 / 2943.930988.
- Verma, A. K., Sarangi, S. and Kolekar, M. (2014). Experimental Investigation of Misalignment Effects on Rotor Shaft Vibration and on Stator Current Signature. *Journal of Failure Analysis and Prevention*, 14 (2), 125-138. Doi. 10.1007 / s11668-014-9785-7.
- Verucchi, C., Bossio, J., Bossio, G. & Acosta, G. (2016). Misalignment detection in induction motors with flexible coupling by means of the estimated torque analysis and MCSA. *Mechanical System and Signal Processing*, 80, 570-581. Doi : 10.1016 / j.ymsp.2016.04.035.
- Wu, J., Zi, Y., Chen, J. & Zhou, Z. (2019). Fault Diagnosis in Speed Variation Conditions via Improved Tachless Order Tracking Technique. *Measurement*, 137, 604-616. Doi. 10.1016/j.measurement.2019.01.086.